Biochimica et Biophysica Acta 1840 (2014) 387–395

Contents lists available at ScienceDirect

Biochimica et Biophysica Acta

journal homepage: www.elsevier.com/locate/bbagen

Step-by-step mechanism of DNA damage recognition by human 8-oxoguanine DNA glycosylase

Alexandra A. Kuznetsova [a,b,1], Nikita A. Kuznetsov [a,b,1], Alexander A. Ishchenko [a,c], Murat K. Saparbaev [c], Olga S. Fedorova [a,b,*]

[a] Institute of Chemical Biology and Fundamental Medicine, Siberian Branch of the Russian Academy of Sciences, Novosibirsk 630090, Russia
[b] Department of Natural Sciences, Novosibirsk State University, Novosibirsk 630090, Russia
[c] Groupe "Réparation de l'ADN", Université Paris-Sud XI, UMR8200 CNRS, Institute Gustave Roussy, Villejuif Cedex F-94805, France

ARTICLE INFO

Article history:
Received 24 April 2013
Received in revised form 23 September 2013
Accepted 25 September 2013
Available online 3 October 2013

Keywords:
Base excision repair
DNA glycosylase
Conformational dynamics
Enzyme kinetics
Human 8-oxoguanine DNA glycosylase

ABSTRACT

Background: Extensive structural studies of human DNA glycosylase hOGG1 have revealed essential conformational changes of the enzyme. However, at present there is little information about the time scale of the rearrangements of the protein structure as well as the dynamic behavior of individual amino acids.
Methods: Using pre-steady-state kinetic analysis with Trp and 2-aminopurine fluorescence detection the conformational dynamics of hOGG1 wild-type (WT) and mutants Y203W, Y203A, H270W, F45W, F319W and K249Q as well as DNA–substrates was examined.
Results: The roles of catalytically important amino acids F45, Y203, K249, H270, and F319 in the hOGG1 enzymatic pathway and their involvement in the step-by-step mechanism of oxidative DNA lesion recognition and catalysis were elucidated.
Conclusions: The results show that Tyr-203 participates in the initial steps of the lesion site recognition. The interaction of the His-270 residue with the oxoG base plays a key role in the insertion of the damaged base into the active site. Lys-249 participates not only in the catalytic stages but also in the processes of local duplex distortion and flipping out of the oxoG residue. Non-damaged DNA does not form a stable complex with hOGG1, although a complex with a flipped out guanine base can be formed transiently.
General significance: The kinetic data obtained in this study significantly improves our understanding of the molecular mechanism of lesion recognition by hOGG1.

1. Introduction

Endogenous and exogenous agents such as highly reactive cell metabolites, external environmental compounds, UV or ionizing irradiation continually damage cellular DNA. The major sources of endogenous DNA damage are reactive oxygen species (ROS). ROS generate a variety of DNA base lesions, including 7,8-dihydro-8-oxoguanine (8-oxoguanine, oxoG), thymine glycol, 2,6-diamino-4-hydroxy-5-formamidopyrimidine (Fapy-G), 4,6-diamino-5-formamidopyrimidine (Fapy-A) and many others [1,2].

Human 8-oxoguanine DNA glycosylase (hOGG1) is a key enzyme responsible for the initiation of base excision DNA repair (BER) of the oxoG residue, a highly mutagenic oxidized DNA base lesion generated by ROS [3–7]. While 8-oxoguanine pairs with cytosine in the Watson–Crick sense, it can also form a Hoogsteen pair with adenine during replication. The oxoG base is then misread as thymine by replicative DNA polymerases leading to oxoG/A base pairing. The resulting oxoG/A mismatch pair gives a G/C → T/A transversion mutation after replication [8].

Human OGG1 recognizes and efficiently excises the oxoG paired with cytosine in double-stranded DNA [6,7,9]. Presumably, the catalytic mechanism of hOGG1 involves an attack on C1′ of the oxoG-containing nucleotide by the ζ-amino group of Lys-249 that leads to the cleavage of the N-glycosidic bond, producing an abasic site (apurinic/apyrimidinic site, AP-site). The incision of the DNA at the 3′-side of AP-sites proceeds via Schiff base formation and subsequent β-elimination reaction leaving a 3′-α,β-unsaturated aldehyde and a 5′-phosphate [10,11].

HOGG1 is a member of the HhH-GPD superfamily of the DNA glycosylases. Other well-studied members of the HhH-GPD superfamily are the bacterial enzymes EndoIII, MutY and AlkA [12–14]. The common feature of these proteins is a helix–hairpin–helix (HhH) motif followed by a Gly/Pro-rich loop and terminating in an Asp residue, which is entirely conserved in HhH-GPD glycosylases. The monofunctional glycosylases of this superfamily AlkA and MutY use the Asp residue as

Abbreviations: 2-aPu, 2-aminopurine; BER, base excision repair; oxoG, 7,8-dihydro-8-oxoguanine; ODN, oligodeoxyribonucleotide; THF, (3-hydroxytetrahydrofuran-2-yl) methyl phosphate

* Corresponding author at: Institute of Chemical Biology and Fundamental Medicine, Siberian Branch of the Russian Academy of Sciences, Novosibirsk 630090, Russia. Tel.: +7 383 363 5174; fax: +7 383 363 5153.
E-mail address: fedorova@niboch.nsc.ru (O.S. Fedorova).

[1] A.A.K. and N.A.K. contributed equally to this work.

0304-4165/$ – see front matter © 2013 Elsevier B.V. All rights reserved.
http://dx.doi.org/10.1016/j.bbagen.2013.09.035

the catalytic nucleophile. In the cases of hOGG1 and EndoIII, which are bifunctional DNA glycosylases, a lysine is present in the active site. The functional role of the invariant Asp residue in the bifunctional glycosylases is not fully understood. In hOGG1 residue Asp-268 cannot directly deprotonate Lys-249, but activates it as a nucleophile, possibly by providing electrostatic stabilization of the active site pocket [15].

In order to identify the amino acid residues involved in the hydrolysis of the N-glycosidic bond Bjoras and coworkers have performed an elegant structure–function study [16]. They have designed separation-of-function mutants and presented biochemical and structural evidence for a monofunctional type of catalysis for hOGG1. Asp-268 was identified as the catalytic residue, while Lys-249 was recognized as a critical amino acid for the specific recognition and final alignment of the oxoG residue during the N-glycosylase reaction [16].

Several three-dimensional structures of hOGG1 and its covalent complexes with DNA have been determined (Fig. 1) [15–21]. These structures reveal that DNA binds to the enzyme in a channel that is nearly charge-neutral with only a single positively charged residue, His-270. This histidine forms the only direct hydrogen bond to the 5′-phosphate of oxoG (Fig. 1A) [15]. In the DNA glycosylase/damaged DNA complexes the DNA is kinked approximately by 70° at the site of the lesion. The damaged nucleotide flips out from the helix to gain access to C1′, a target for nucleophilic attack. This process is accompanied by the insertion of Tyr-203, Asn-149, Arg-154 and Arg-204 amino acid residues into the resulting void in the DNA (Fig. 1B). Tyr-203 inserts into the space between C (opposite oxoG) and the base on its 5′-side. Residues Arg-154 and Arg-204 are involved in hydrogen-bonding interactions with the N_3- and O_2-atoms of the unpaired cytosine base from different sides of its plane. In addition, Asn-149 forms a hydrogen bond between the amide carbonyl atom of the side chain moiety and the amino group of the cytosine [17]. The amino acid residues Phe-319, Cys-253, Gly-42, Gln-43, Phe-45 and Gln-315 form the 8-oxoguanine binding pocket. In the active site, the phenyl ring of Phe-319 makes a face-to-face π–π contact with the oxoG nucleobase. Phe-319 and Cys-253 interact with the opposite π-face of oxoG, sandwiching the base in the active site. The side-chain carbonyl of Gln-315 forms hydrogen bonds with both N1 and N2H of the oxoG base. The N7-H group of the oxoG base donates a hydrogen bond to the main chain carbonyl of Gly-42. Gln-43 forms the distant wall of the binding pocket and has no direct contact with the oxoG base.

Non-specific binding of the enzyme to the non-damaged DNA (G-ligand) leads to destabilization of the double helix. The kink in the DNA helix in the covalently linked disulfide complex (PDB ID: 1YQK) [19] between hOGG1 and G-containing DNAs was found to be 80°. According to the structure of the complex of hOGG1 with a non-damaged DNA the G base is flipped out into the exo-site which is located at a distance of about 5 Å from the enzymes' catalytic pocket. However, the G-base has the possibility to interact directly with the Phe-319 and

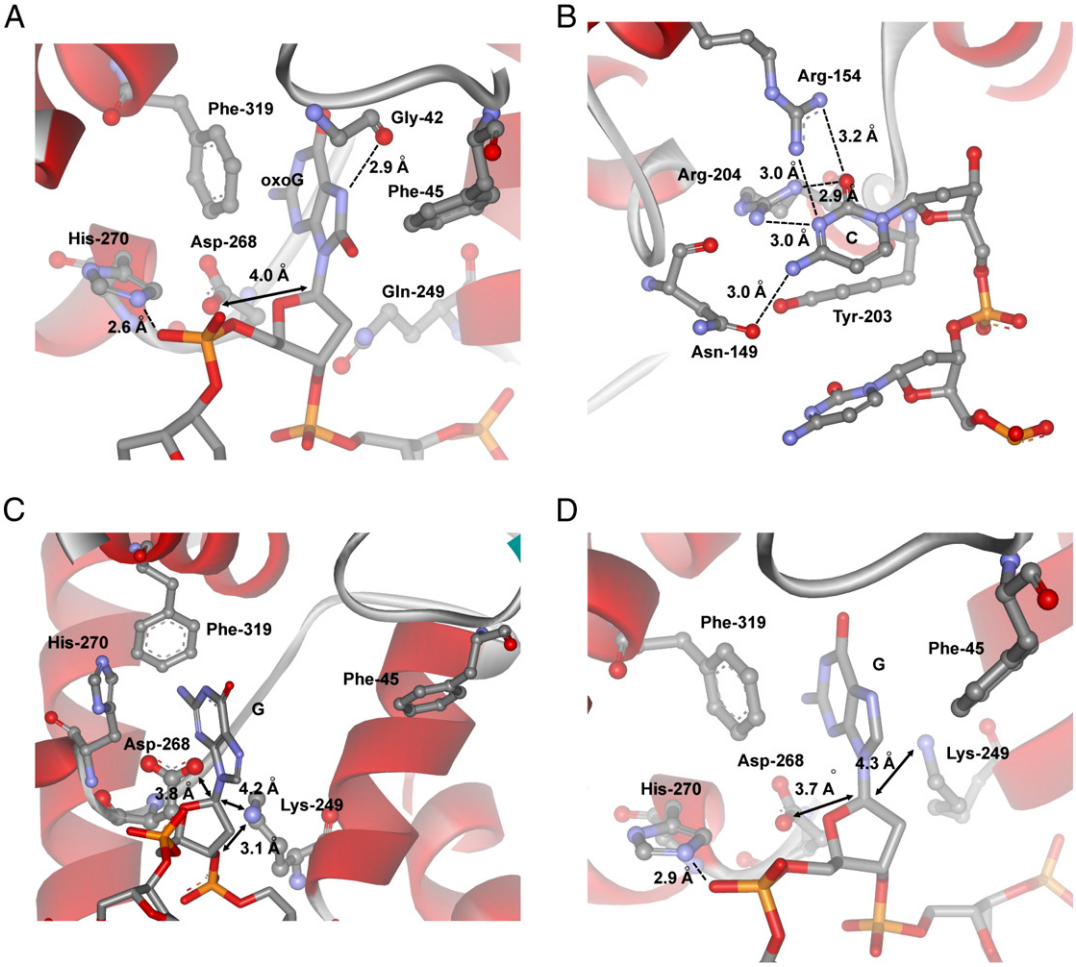

Fig. 1. Close-up view of the important contacts for the recognition oxoG/C or G/C base pairs in the active site of the hOGG1 complexes with DNA; H-bonds are shown by the dashed line, the distances between Asp-268 Oδ1 and C1′-atom of the ribose, Lys-249 Nζ and C1′-atom or O3′-atom of the ribose are shown: (A) the lesion recognition complex of hOGG1 bound to DNA with the oxoG base inserted in the active site (PDB ID: 1YQR, [19]), (B) specific contacts of enzyme with the cytosine which is located opposite to oxoG base (PDB ID: 1EBM, [17]), (C) the complex of hOGG1 bound to the DNA with the G base inserted in the exo-site (PDB ID: 1YQK, [19]), (D) the complex of hOGG1 bound to the DNA, with the G base inserted in the active site (PDB ID: 3IH7, [21]).

His-270 of the active site (Fig. 1C). In the recent paper from Verdine's laboratory, the authors describe the structure of another covalently linked disulfide complex (PDB ID: 3IH7) (Fig. 1D) [21] of hOGG1 with the non-damaged DNA. They showed that the non-damaged G base is located in the active center of hOGG1 approximately in the same position as the oxoG base in the lesion recognition complex (Fig. 1A), but hOGG1 fails to catalyze excision of the normal nucleobase. These data show that the lesion recognition system of hOGG1 is very sensitive to the structural features of the DNA that can lead to rejection of non-damaged DNA in the last steps of the protein/DNA interaction.

Despite detailed knowledge on the chemical mechanisms of the main steps of the repair processes and the atomic structures of the complexes of enzyme with damaged and non-damaged DNA it is still unclear how the search for the lesion proceeds and what the initial steps of the enzyme/DNA interactions are that lead to discrimination of G from oxoG. In addition, the elucidation of the exact functional roles of Asp and Lys residues in the catalytic steps of the repair process is necessary.

The interaction of hOGG1 with the DNA duplex may consist of multiple steps, including the encounter complex formation, sliding/rotation the enzyme along the DNA chain into a specific position, lesion recognition, catalytic steps and the release of product from the enzyme complex [22,23]. It is obvious that mutual structural adjustment of hOGG1 and the DNA is responsible for the high specific affinity of the enzyme and that there are some crucial conformational changes, which determine whether the following steps of the enzyme/substrate interaction will proceed.

In the present work, we aim to gain a better understanding of the recognition process of specific oxoG- and AP-substrates and non-damaged G-containing ligands by hOGG1. To this end the hOGG1 mutants Y203W, Y203A, H270W, F45W, F319W and K249Q, which contain substitutions of functionally important amino acids, have been constructed. Real time conformational rearrangements of the enzyme and the DNA in the course of their interactions were visualized using tryptophan (Trp) and 2-aminopurine (2-aPu) as fluorescence reporters. Using pre-steady state stopped-flow measurements the reaction's progress from the substrate binding to the product release and the catalytic turnover has been monitored, as described recently [22–24]. In most cases, specific amino acids were substituted with fluorescent Trp, which permits monitoring of the conformational transitions in the vicinity of these residues. These studies allowed: (i) to observe conformational changes of the enzyme and the substrates in real time during lesion search, damaged base recognition and catalysis; (ii) to specify the role of certain catalytically important amino acids during enzymatic pathway; and (iii) to describe step-by-step their participation in the sequential mechanism of oxidative DNA lesion recognition and processing by hOGG1.

2. Material and methods

2.1. Enzymes and oligodeoxynucleotides

Isolation of the wild-type and mutant hOGG1 proteins was described previously [22]. Site-directed mutations Y203W, Y203A, H270W, F45W, F319W or K249Q within the hOGG1 coding sequence were generated using a site-directed mutagenesis kit (QuikChange XL, Stratagene) according to the manufacturer's protocol.

The sequences of ODNs used in this work are listed in Table 1. The ODNs were synthesized by established phosphoramidite methods using an ASM-700 synthesizer (BIOSSET Ltd., Novosibirsk, Russia) in the Laboratory of Bionanotechnology of ICBFM. Phosphoramidites were purchased from Glen Research (Sterling, VA). ODN duplexes were prepared by annealing modified and complementary strands at a 1:1 molar ratio.

Table 1
Sequences of oligodeoxynucleotides used in this work.

Shorthand	Sequence
oxoG	d(CTCTC(oxoG)CCTTCC)
oxoG-aPu	d(CTCTC(oxoG)(2-aPu)CTTCC)
AP	d(CTCTC(AP)CCTTCC)
AP-aPu	d(CTCTC(AP)(2-aPu)CTTCC)
G	d(CTCTCGCCTTCC)
G-aPu	d(CTCTCG(2-aPu)CTTCC)
C	d(GGAAGGCGAGAG)
CCG	d(GGAAGCCGAGAG)

2.2. Stopped-flow fluorescence measurements

Stopped-flow measurements with fluorescence detection were carried out essentially as described previously [22,23] using a model SX.18MV stopped-flow spectrometer (Applied Photophysics Ltd., Leatherhead, UK). To detect intrinsic Trp fluorescence only, $\lambda_{ex} =$ 290 nm was used for excitation and the emission at $\lambda_{em} > 320$ nm was detected as transmitted by a Schott filter WG320 (Schott, Mainz, Germany). If 2-aPu was present in the ODNs, $\lambda_{ex} = 310$ nm was used to excite 2-aPu residues, and their emission was followed at $\lambda_{em} > 370$ nm (Corion filter LG-370). The concentration of hOGG1 in all experiments with Trp fluorescence detection was 1 μM, and the concentrations of ODN substrates were varied from 0.5 to 2 μM. The concentration of the substrates containing 2-aPu in the experiments with 2-aPu fluorescence detection was 1 μM, and the concentrations of hOGG1 protein were varied from 0.5 to 2 μM. Typically, each trace shown is the average of four or more individual experiments. All experiments were carried out at 25 °C in a buffer containing 50 mM Tris–HCl, pH 7.5, 50 mM KCl, 1 mM EDTA, 1 mM DDT and 9% glycerol (v/v).

2.3. Nonlinear fitting of the stopped-flow data

All stopped-flow traces were modeled after correction for internal absorption and bleaching. A simplified analysis of the fluorescent traces for G- and AP-containing DNA was done as a sum of exponentials according to Eq. (1):

$$F_c = F_b + \sum_{i=0}^{N} A_i \times \exp(-k_i \times t) \quad (1)$$

where i is the index number, A_i is a coefficient, and k_i is the observed rate constant.

2.4. Global nonlinear simulation fitting of the stopped-flow data

The stopped-flow data obtained for enzyme interaction with the oxoG-containing DNA fitted to Scheme 1, containing n reversible, m irreversible steps, and an enzyme/product complex equilibrium step.

All stopped-flow traces were accurately modeled by numerical fitting using DynaFit software (BioKin, Pullman, WA) [25] as described [22,23] (for details see Supplementary material).

3. Results

3.1. Mutants' design rationale

The amino acids Lys-249, Tyr-203, Phe-45, Phe-319 and His-270, which are important for binding and catalysis, were substituted to obtain the following hOGG1 mutants Y203W, Y203A, H270W, F45W,

$$E + S \rightleftarrows (E{\bullet}S)1 \rightleftarrows \bullet\ \bullet\ \bullet \rightleftarrows (E{\bullet}S)n \longrightarrow (E{\bullet}P)1 \longrightarrow \bullet\ \bullet\ \bullet \longrightarrow (E{\bullet}P)m \rightleftarrows E + P$$

Scheme 1. Total sequential kinetic mechanism of the enzyme-substrate interactions.

F319W and K249Q. It had been shown that these amino acids directly interact with the extrahelical damaged and/or non-damaged base and/or participate in the formation of specific contacts between DNA and hOGG1 (Fig. 1) [17,19,20].

Tyr-203 is one of the four amino acids of hOGG1 (Tyr-203, Asn-149, Arg-154 and Arg-204) that fill the void in the DNA substrate after flipping out of the damaged base [17]. In the catalytically active complex (Fig. 1B) the aromatic ring of Tyr-203 is wedged into the space between the cytosine placed opposite to oxoG and the base on its 5′-side thereby unstacking the two bases and creating a sharp kink in the DNA.

Phe-45 is located in the active site of the enzyme near the flipped out oxoG base (Fig. 1A). The distance between the aromatic ring of the Phe-45 and the flipped out oxoG plane is almost 2-fold less than that for non-damaged G if it is located in the exo-site [17,19] (Fig. 1C).

Phe-319 is involved in stacking with the oxoG base in the active site (Fig. 1A). However, in the complex with a non-damaged duplex when the G base is located in the exo-site (Fig. 1C) Phe-319 contacts the G base in an orientation perpendicular to its plane [19]. It was shown earlier [26] that Phe-319 is essential to form the functional 8-oxoG-binding pocket, because the substitution of the Phe-319 by Ala decreased the DNA glycosylase activity, but increased the AP-lyase activity of hOGG1.

His-270 interacts with the 5′-phosphate group of the extruded nucleotide in the case of both oxoG and G bases when they are placed in the active site (Fig. 1A and D), and stacks with the non-damaged G base placed in the exo-site (Fig. 1C). Structural studies support the idea that the H270A mutation diminishes the binding affinity to DNA, which leads to a destabilization of the lesion recognition complex [20]. It was shown [26] that mutation H270A dramatically inactivates the enzyme toward the oxoG-substrate, but retains activity for AP-substrates comparable with the activity of the wild-type enzyme.

The substitution of Lys-249 by Gln completely inactivates both N-glycosylase and AP-lyase activities of the enzyme. Nevertheless, mutant K249Q retains the ability to recognize DNA lesions and tightly binds oxoG- and THF-containing DNA [11,15,27].

3.2. Non-specific DNA binding (G-DNA)

The fluorescence traces obtained for hOGG1 WT and mutants, even for mutants, which contain an additional tryptophan residue, revealed a slight decrease of the magnitude of the intrinsic Trp fluorescence during enzyme binding to G-DNA (Supplementary Fig. S1). Introduction of an additional Trp residue did not result in an increase of the total fluorescence intensity. We suggest that hOGG1 WT and mutants do not go through significant conformational rearrangements when interacting with G-DNA in a non-specific manner. At the same time, the significant growth of the 2-aPu fluorescence intensity unambiguously indicates that the Watson–Crick and/or stacking interactions in the primary non-specific enzyme/G-DNA complex (Fig. 2) are destabilized, possibly in conjunction with flipping out of the G residue into the exo-site [23]. The kinetics were described using Eq. (1), where $N = 2$ (2-equilibrium binding mechanism). The rate constants of the first and the second phase were determined for hOGG1 WT and all mutants (Supplementary Table S1 and Supplementary Fig. S2). The difference in the magnitude of 2-aPu fluorescence intensity can be attributed to the difference in the abilities of hOGG1 WT and the mutants to bind non-damaged DNA and to different levels of distortion of the double helix.

3.3. Interaction with DNA containing an AP-site

Upon the interaction with the AP/C-substrate the intrinsic Trp fluorescence of the hOGG1 mutants decreases slowly over a 10 s time interval (Fig. 3A) in agreement with previous data obtained for the WT enzyme [22]. Since hOGG1 has been reported to process AP-sites by a β-elimination mechanism with very low efficiency, such a decrease of the Trp fluorescence should reflect only the DNA binding step [4,7]. The observed rate constants (Supplementary Table S2) derived from the analysis of the Trp fluorescence data (Supplementary Fig. S3) using Eq. (1), where $N = 1$, are essentially the same for hOGG1 WT and all mutants except for hOGG1 H270W (no fluorescence changes at all) and hOGG1 K249Q (the fluorescence decrease is 1.7-fold slower than that of WT enzyme).

AP-aPu/CCG-substrate binding and abasic void filling by hOGG1 also leads to detectable 2-aPu fluorescence changes demonstrating the conformational transitions of DNA (Fig. 3B). The slight increase of the 2-aPu

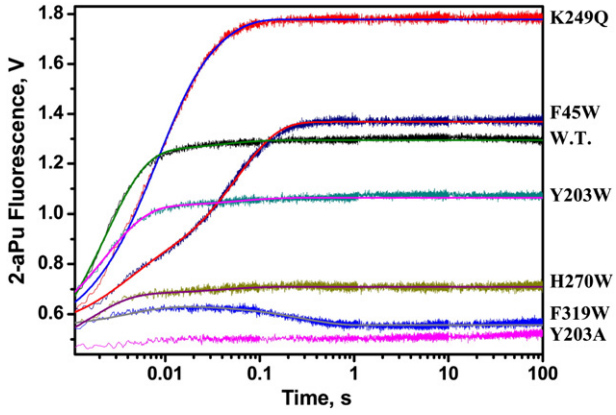

Fig. 2. Conformational changes of the G-ligand during interaction with WT and mutant forms of hOGG1 studied using 2-aPu fluorescence. The concentrations of hOGG1 and G-ligand were 2 μM and 1 μM, respectively.

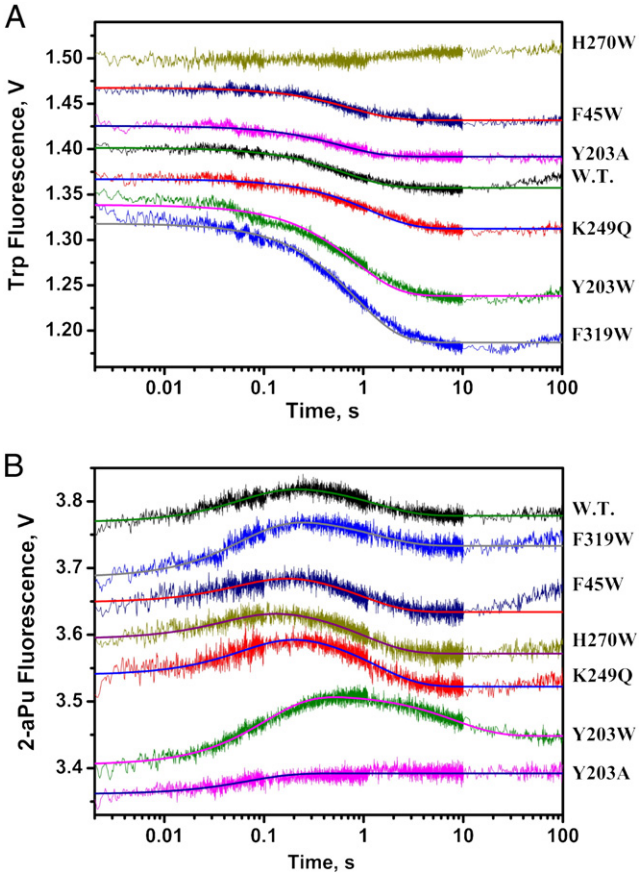

Fig. 3. Experimental fluorescence traces characterizing enzyme kinetics and the conformational changes in hOGG1 (A) and AP-substrate (B) during their interaction. The concentrations of hOGG1 and AP-substrate were 2 μM and 1 μM, respectively.

fluorescence intensity (within 100 ms) for hOGG1 WT and all mutants should be associated with an increase in hydrophilicity of the environment around the 2-aPu residue. Possibly this is due to a partial melting of the duplex and/or interactions with the hydrophilic amino acids Arg-154, Arg-204 and Asn-149. It should be noted that Asn-149 is located at 3.5 Å from the 3′-side base (2-aPu in our case) in the THF-ligand/hOGG1 complex [28]. At the same time the incorporation of the Tyr-203 residue perturbs the base which is complementary to the 2-aminopurine.

Processing of the 2-aPu fluorescence data was done using Eq. (1) with $N = 2$. The observed rate constants of the first stage of the signal increase k_1^{obs} vary in the rather narrow range from 9.6 s^{-1} to 21.8 s^{-1} for all proteins (Fig. 3B and Supplementary Fig. S4). The second stage, which leads to the decrease of the fluorescence intensity, is possibly associated with the transition of the 2-aPu residue to a more hydrophobic environment. The observed rate constants k_2^{obs} of this stage for hOGG1 WT and H270W, F45W, F319W, K249Q mutants lie in the range from 0.74 s^{-1} to 1.03 s^{-1}, whereas for mutant Y203W this value is 0.12 s^{-1}, which is six times lower than that of WT. As shown in Fig. 3B, the Y203A mutant has lost the ability to process the second step of AP-substrate binding supporting the idea that the nature of this process is the complete insertion of Tyr-203 into the DNA helix.

3.4. Interaction with oxoG-substrate

3.4.1. Wild-type hOGG1

A discernible decrease of the hOGG1 Trp fluorescence signal (during 10 s) was observed in the course of the interaction between hOGG1 WT and duplex DNA containing single oxoG residue (Fig. 4A). It was shown in our previous studies [22] that this phase consists of three steps which were attributed to the specific enzyme/DNA complex formation. The subsequent increase of the Trp intensity should be due to the chemical steps and the process of dissociation of the enzyme/product complex.

Detection of the 2-aPu fluorescence demonstrated an increase of the intensity during the first 20 ms. In this time range the oxoG residue flips out from the duplex, leaving a void in the DNA helix. The subsequent insertion of the amino acid residues Tyr-203, Asn-149, Arg-154 and Arg-204 into this void resulted in a noticeable two-step decrease in 2-aPu fluorescence during the next period 20 ms–100 s. The catalytic steps and the dissociation of the enzyme/product complex resulted in an increase in the 2-aPu fluorescence intensity because of the transition of the 2-aminopurine to a more hydrophilic environment (Fig. 4B) at times >100 s. The minimal kinetic scheme describing the observed changes of the 2-aPu fluorescence intensity was identical to that proposed earlier for the description of Trp fluorescence changes (Scheme 2) [23].

Scheme 2 includes three reversible steps that characterize the substrate binding followed by two irreversible chemical steps and, after that, by a reversible step of the product release from the enzyme/product complex. The rate and equilibrium constants obtained from global fitting of the experimental data at different concentrations of the enzyme and oxoG-DNA substrate (Supplementary Fig. S5) are presented in Supplementary Table S3 [22,23].

3.4.2. Y203A

It follows from Fig. 5 and Fig. S5A and S5B that mutation Y203A leads to the nearly complete loss of the N-glycosylase and AP-lyase activities. This result is in accord with the negligible decrease of Trp fluorescence and the absence of any changes in 2-aPu fluorescence signal until 500 ms (Fig. 4A, B). Only a small quantity of the AP-product was detected at $t > 500$ s (Fig. 5). Therefore, mutation Y203A results in the inability of the enzyme to recognize the damaged base and to induce both the initial melting and subsequent oxoG base flipping.

3.4.3. Y203W

The Trp fluorescence curves obtained for the interaction of hOGG1 Y203W with oxoG-substrate display an additional decrease of Trp-signal in the time range 1–20 s as compared with hOGG1 WT (Fig. 4A).

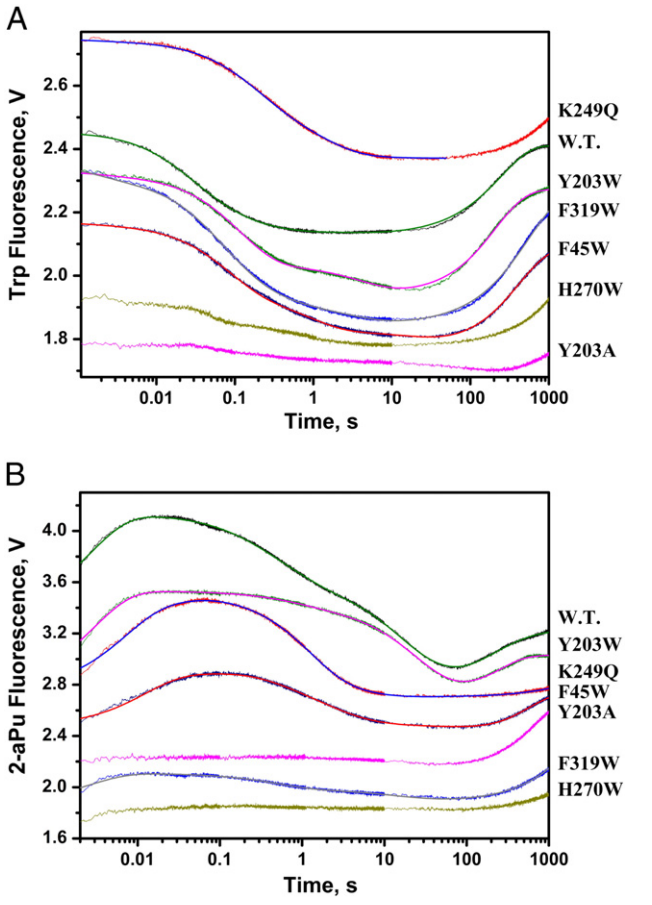

Fig. 4. Experimental fluorescence traces characterizing the enzyme kinetics and the conformational changes of hOGG1 (A) and oxoG-substrate (B) during their interactions. The concentrations of hOGG1 and oxoG-substrate were 2 μM and 1 μM, respectively.

Such a change in the fluorescence curve indicates that specifically Trp-203 is responsible for this change. It is reasonable to suggest that Trp-203 is involved in oxoG recognition and the insertion of this residue into the DNA duplex takes place in the time range 1–20 s. This Trp fluorescence behavior permits concluding that the amino acids Asn-149, Arg-154, Arg-204 and Tyr-203 are sequentially inserted in the DNA void, and that the last inserted amino acid is Tyr-203.

Comparison of the 2-aPu fluorescence changes (Fig. 4B) and the PAGE reaction products accumulation for ^{32}P-labeled oxoG-substrate (Fig. 5) reveals approximately the same time ranges for the DNA conformational transitions and the catalytic steps.

The Trp and 2-aPu fluorescence kinetics, obtained at different concentrations of oxoG-substrate (Fig. S5A) and hOGG1 Y203W (Fig. S5B), respectively, are described by the same kinetic scheme as for hOGG1 WT (Scheme 2). The results of global fitting are presented in Table S3. Both Trp and 2-aPu reveal a slight decrease in the efficiency of enzyme/substrate complex formation (as is evident by comparing K_1, K_2 and K_3) as well as the rates of the catalytic steps (compare the values of k_4 and k_5). Therefore, mutation Y203W does not reduce the enzymatic activity of hOGG1, and Y203 is important for both lesion recognition and formation of the catalytic competent state.

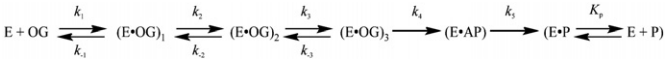

Scheme 2. Kinetic mechanism of hOGG1 processing of the oxoG-substrate. E, hOGG1;OG, oxoG-substrate; (E·OG)n and E·AP, different enzyme/substrate complexes; P, reaction product; E·P, enzyme/product complex; k_i and k_{-i}, are the individual rate constants.

3.4.4. H270W

His-270 plays a crucial role in the formation of the catalytically active complex with the oxoG-substrate [20,26]. The His-270 imidazole moiety forms a H-bond with the 5′-phosphate of the damaged nucleotide [17]. The His-270–Asp-322 interaction serves for keeping the active site open to facilitate insertion of the lesion nucleobase. As is seen from Fig. 5, hOGG1 H270W lost completely the catalytic activity toward the oxoG-substrate. The very slight decrease of Trp fluorescence supports the suggestion that the mutant hOGG1 H270W cannot appreciably bind the oxoG-containing DNA (Fig. 4A). This suggestion is also supported by the absence of any changes in the 2-aPu fluorescence curve (Fig. 4B). Structural data [20] obtained for the complex formed between hOGG1 H270A mutant and oxoG-containing DNA reveal that this mutation diminishes binding by the preventing the direct interaction stabilizing the lesion-recognition complex.

3.4.5. F319W

In the active site of free hOGG1, Phe-319 stacks with His-270 [18]. When the catalytically active complex is formed, the Phe-319 aromatic ring forms a π–π stacking interaction with oxoG [17].

As follows from the PAGE analysis of the abasic and nicked product accumulation, presented in Fig. 5, hOGG1 F319W possesses both N-glycosylase and AP-lyase activities, but both are approximately 2–3 times lower than in the case of the WT enzyme. The Trp fluorescence intensity for hOGG1 F319W decreases more gradually than that in the case of hOGG1 WT (Fig. 4A). This means that the catalytically competent enzyme/substrate complex forms more slowly than in the case of WT enzyme.

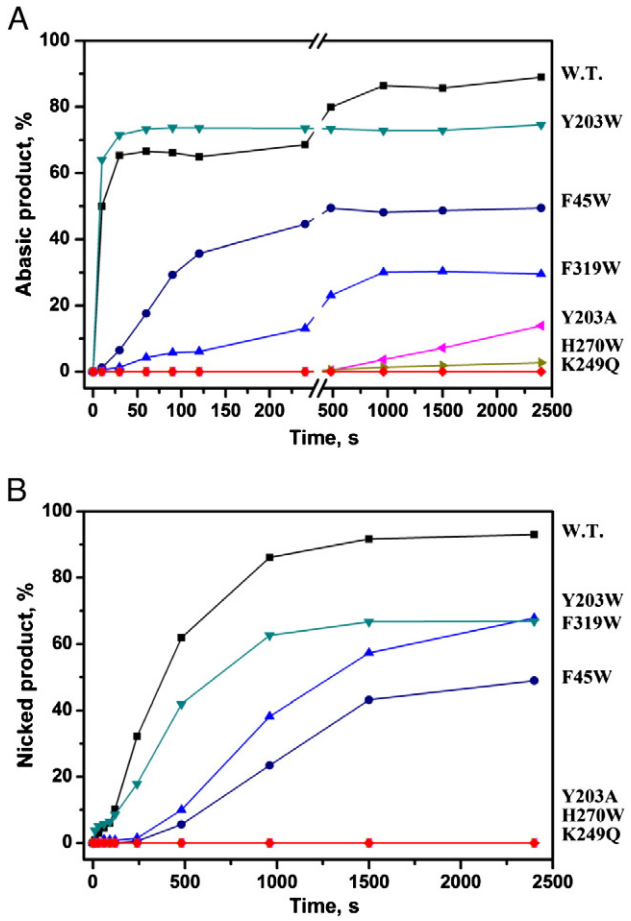

Fig. 5. Time course of the accumulation of the abasic (A) and nicked (B) products as detected in PAGE experiments. The concentrations of hOGG1 and oxoG-substrate were 2 μM and 1 μM, respectively.

The Trp and 2-aPu fluorescence kinetics, obtained at different concentrations of oxoG-substrate (Fig. S5C) and hOGG1 F319W (Fig. S5D), respectively, are described in Scheme 2. The global fitting of Trp fluorescence curves according to Scheme 2 shows (Supplementary Table S3) that this mutant forms a complex with the oxoG-substrate more effectively (compare K_{bind} and $K_1 \times K_2 \times K_3$ values),but catalytically it is less active (compare k_4 and k_5) than the WT enzyme. The main effect of F319W substitution is observed on the second and third steps of binding. These data permit to conclude that the interaction with the Phe-319 residue occurs in these equilibrium steps resulting in the formation of the catalytically active complex.

The 2-aPu fluorescence shows a slight increase of the intensity up to 10 ms (Fig. 4B). This modest increase of the 2-aPu fluorescence indicates inefficiency of the flipping out process of the damaged base. In the time range 10–100 ms the 2-aPu fluorescence signal is not changed and slowly decreased in the range 100 ms–100 s. This 2-aPu signal decrease up to 100 s might be due to the inefficient void-filling by the Arg-154, Arg-204, Tyr-203 and Asn-149 residues and the slow formation of the catalytically active complex. It should be noted that the forward and the reverse rate constants of the second and third binding steps are larger than the rate constants for the WT enzyme indicating instability of the intermediate complexes (Supplementary Table S3).

The process of stacking formation between oxoG base and Trp-319 residue in hOGG1 F319W could be not as effective as in the case of the Phe-319 in hOGG1 WT. This would lead to lower fraction of this intermediate formation and only slight 2-aPu fluorescence changes, as observed (Fig. 4B).

3.4.6. K249Q

PAGE analysis of the abasic and nicked product accumulation (Fig. 5) shows that hOGG1 K249Q lost both the N-glycosylase and AP-lyase activities. The shapes of the fluorescence kinetic curves characterizing hOGG1 K249Q and oxoG-DNA conformational changes in the course of their interactions differ significantly from those obtained for the WT enzyme. The formation of the specific complex with hOGG1 K249Q detected by Trp fluorescence proceeds more slowly (up to 10 s) than in the case of hOGG1 WT (Fig. 4). The increase of the 2-aPu fluorescence corresponding to the duplex distortion and flipping out of the oxoG base occurs also slower and takes approximately 100 ms instead of 20 ms for the WT enzyme. The Trp and 2-aPu fluorescence kinetics, obtained at different concentrations of oxoG-substrate (Fig. S5E) and hOGG1 K249Q (Fig. S5F), respectively, are described by a modified Scheme 2 with removed irreversible chemical steps. As is seen from the data of Table S3, k_1 is 4 times smaller than for hOGG1 WT. The next stage, where the 2-aPu fluorescence is decreased, presumably, due to the insertion of the amino acid residues Tyr-203, Asn-149, Arg-154 and Arg-204 in the DNA double helix, proceeds faster than in the case of hOGG1 WT and is completed up to 10 s (k_3 is 54 times larger). The equilibrium stability constant of $(E{\cdot}OG)_3$ complex ($K_1 \times K_2 \times K_3$) is 7 times smaller compared with the WT enzyme (Supplementary Table S3).

These results allow suggesting that the conformation of the active site of hOGG1 K249Q is less appropriate for the recognition of the specific DNA substrate and this process proceeds less efficiently than in the case of WT enzyme. For this mutant full adaptation of the DNA helix structure to the catalytically active form is not possible. Therefore, mutation K249Q reduces DNA binding with the enzyme in complete agreement with the data [16].

3.4.7. F45W

The substitution of Phe-45 by Trp leads to a decrease of the catalytic activity of the enzyme as is seen from the data for the PAGE analysis (Fig. 5). The time-dependent Trp and 2-aPu fluorescence curves show a slowing down of the DNA binding step up to 30–40 s (Fig. 4). Fluorescence kinetics, obtained at different concentrations of the oxoG-substrate or hOGG1 F45W (Fig. S5G and S5H, respectively), is

described by the same Scheme 2. The comparison of the equilibrium constants presented in Supplementary Table S3 reveals that the equilibrium constants differ from the equilibrium constants for the WT enzyme (K_3 0.02 vs. 0.17 for Trp and 1.3 vs. 7.7 for 2-aPu). The decrease of the reaction rate constant k_3 of the third binding step, which is responsible for the final adjustment of the enzyme/substrate complex to the catalytically active state, may result from local reconstruction of the active site structure because of the substitution of Phe with bulky Trp. Nevertheless, the catalytic activity of hOGG1 F45W was similar to that of hOGG1 WT (k_4 and k_5 rate constants in Supplementary Table S3).

4. Discussion

The results of the kinetic analysis clearly demonstrate that hOGG1 is able to control the substrate specificity by a multistep mechanism (Scheme 3) of specific site recognition accompanied with the conformation changes both in the enzyme and in the DNA-substrate.

On the basis of an analysis of the fluorescence kinetic data it is plausible to conclude that the first step of the oxoG-DNA binding process corresponding to the formation of complex $(E{\cdot}OG)_1$ on the time scale $\leq$ 20 ms represents non-specific binding. The data obtained

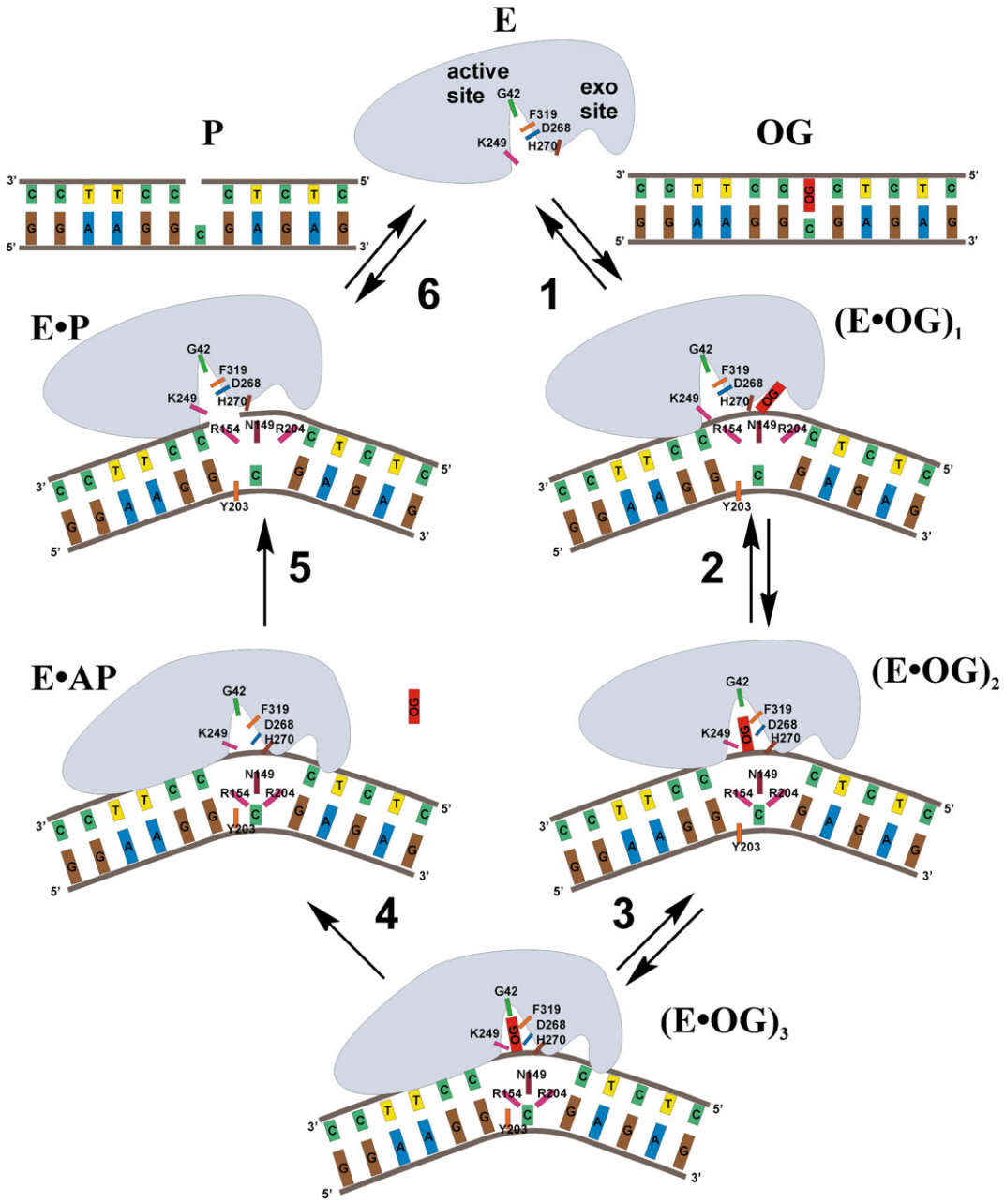

Scheme 3. Step-by-step kinetic mechanism of hOGG1 processing of the oxoG-substrate. Molecular processes during the course of the reaction:

Step 1 C base pulling by Arg-154/Arg-204, pushing of Tyr-203 into DNA helix, electrostatic interaction between Lys-249 and the damaged nucleotide, oxoG flipping out in the exo-site, interaction of His-270 with the everted base;
Step 2 oxoG flipping out in the active site, oxoG stacking with Phe-319, His-270 interaction with phosphate group of the everted nucleotide, formation of hydrogen bonds between Arg-154, Arg-204, Asn-149 and C base;
Step 3 full insertion of Tyr-203 in DNA helix, oxoG interaction with Gly-42;
Step 4 N-glycosidic bond cleavage by Asp-268;
Step 5 β-elimination reaction by Lys-249;
Step 6 dissociation of the enzyme/product complex.

for both hOGG1 Y203A and Y203W show that the distortion of oxoG-containing DNA proceeds with direct participation of Tyr-203. At the same time mutation Y203W shows that the full insertion of the Trp-203 residue into DNA takes place at a later stage of the interaction process ($t > 1$ s). This finding leads to the conclusion that a different initial protein/DNA interaction should be realized with decreased Trp fluorescence at $t < 1$ s. It is reasonable to suggest that this occurs due to the H-bond formation between hOGG1 amino acids Arg-154 and Arg-204 and the cytosine base located opposite the oxoG base. These interactions "*pull out*" *the cytosine* base toward the minor DNA groove and result in the *destabilization of the H-bonds between cytosine and oxoG bases*. A significant dependence of the enzyme activity upon the nature of the base opposite to the lesion can prove such an assumption. Cytosine is the preferred opposite base, as compared with A, G, or T because only C is able to form H-bonds with the Arg-154 and Arg-204 side chains [7,23]. This is in agreement with the observation that the substitution of Arg-154 residue by His [29] in hOGG1 or the presence of Met, playing the same structural role in CacOgg as Arg-154 [30], leads to a significant decrease of the selectivity versus the base opposite to the lesion.

In the case of the Y203A mutant, 2-aPu fluorescence does not increase at all in the first step (Fig. 4B). Therefore, the *partial pushing of Tyr-203 into the DNA duplex* slightly destabilized by Arg-154 and Arg-204 is also required in this step. The possible function of Tyr-203 residue in the search for damaged bases is as a "lesion-sensor needle" similar to the Phe-110 side chain of the Fpg protein from *Escherichia coli* [31,32].

The insertion of Tyr-203 in the duplex strand proceeds with the involvement of His-270, which participates in the initial DNA helix distortion. The substitution of His-270 leads to a slight increase of the 2-aPu fluorescence observed for the H270W mutant up to 10 ms, which supports this hypothesis. Separation of the DNA chains would facilitate not only the partial insertion of Tyr-203, but also the *flipping of oxoG from the DNA chain into the exo-site*, leaving a void accessible for water molecules. Finally, it is seen from the data for hOGG1 K249Q, that residue *Lys-249 is important for the initial stage* of the formation of primary complex hOGG1/DNA in agreement with [16], where Lys-249 was shown to be critical for the specific recognition and final alignment of the oxoG containing DNA.

The second DNA damage recognition step (Scheme 3) corresponds to the formation of complex $(E{\cdot}OG)_2$ and to the time range from about 20 ms to 1 s. During this step the *oxoG base is everted into the active site* and fixed there due to π–π *stacking with the aromatic ring of Phe-319*. This conclusion results from the changes in 2-aPu fluorescence, recorded for F319W hOGG1 (Figs. 4B and S5D). Analysis of the X-ray structure [20] shows that apart from Phe-319 also other residues (His 270 and Gln-315) recognize the oxoG nucleotide in the active site. The absence of *H-bonding of the His-270 with the 5′-phosphate group* of the damaged nucleotide leads to substantial loss of both DNA-binding and DNA-glycosylase activities (this study for hOGG1 H270W and Ref. [26]). After full flipping out of the oxoG base from the DNA helix the *formation of contacts of Arg-154, Arg-204 and Asn-149 with the opposite cytosine base* should be completed.

The third DNA damage recognition step (Scheme 3), corresponding to the formation of the complex $(E{\cdot}OG)_3$, proceeds in the time range of 1–20 s. Most likely, this step is connected with the *full insertion of Tyr-203 in the duplex* as follows from the data for hOGG1 Y203W (Figs. 4B and S5B). Kinetic data obtained in this study for the mutant hOGG1 F45W shows that the third binding step is responsible mainly for the *final adjustment of the enzyme/substrate complex* to achieve the catalytically active state.

We should also comment on the role of Lys-249 and Asp-268 in the catalytic activity of hOGG1. The commonly accepted dogma of the chemical mechanism of hOGG1 is that the Lys-249 side chain amino group participates both in the N-glycosidic bond cleavage and in the β-elimination reaction. This assumption is based on the finding that Lys-249 forms a Schiff base with the C1′-atom of the ribose. Our data suggest that the Lys-249 residue directly participates in the process of DNA distortion and the flipping out of the oxoG base, presumably, due to the initial electrostatic interactions with the DNA phosphate groups. Moreover, such interactions were observed in the crystal structure of the complex between hOGG1 and non-damaged DNA (Fig. 1C) [19] and were detected by chemical cross-linking between Lys-249 and the phosphate located on the 3′-side to the oxoG residue [33]. The loss of these electrostatic interactions in the K249Q mutant leads to the disruption of specific contacts in the active site of the enzyme and the absence of catalytic activity.

Recently it was shown [16] that Asp-268 is involved in base excision catalysis in the double mutant K249C C253K of hOGG1. According to this data the formation of the Schiff-base between Lys-249 and C1′-deoxyribose of the damaged nucleotide should occur after the cleavage of the N-glycosidic bond with the damaged base as it was shown for another member of HhH-GPD family MutY [34,35]. Therefore, based on all of these data, the assumption was made that the K249Q mutation obliterates the base excision activity by disruption of the local structure of the active site in the lesion recognition complex but not due to the loss of the nucleophilic amino group of Lys-249.

Analysis of the structural data shows that in the complexes of the monofunctional DNA glycosylases AlkA from *Escherichia coli* (PDB ID: 1DIZ) [36] and MutY from *Bacillus stearothermophilus* (PDB IDs: 3FSQ and 3G0Q) [37] with DNA the distances between the catalytic Asp residue and C1′-atom of the flipped out damaged nucleotide are 3.2 Å. As shown in Fig. 1A the distance between Asp-268 of hOGG1 K249Q and C1′-atom of the oxoG nucleotide is 4.0 Å and the hydrolysis of the N-glycosidic bond in this case is not favorable. The distance between Asp-268 of hOGG1 WT and C1′-atom of non-damaged G nucleotide (Fig. 1D) is also too large (3.7 Å) to achieve the catalytic competent state, which explains the inability of the enzyme to remove the G base even if it is placed in the active site.

Another comment relates to the structure of hOGG1 with G-containing non-specific DNA. It was shown recently [21] that the G base can be placed in the active site of hOGG1 in the same mode as the oxoG base and the position of the Lys-249 is the same in these two cases. Nevertheless, the catalytic steps occur only with oxoG, but not with G-containing DNA. It should be noted that the final discrimination of G versus oxoG is realized due to H-bond formation of the oxoG N–H with the main chain carbonyl of Gly-42. However, this contact is limited by conformational mobility of the oxygen atom of the amide bond of Gly-42. It is clear that this contact is formed after the insertion of oxoG into the active site and stabilizes the flipped out state. This state allows adjusting the distance between the catalytic amino acid and C1′-atom of the damaged base.

As is seen from Fig. 2, in the case of non-specific G-containing DNA, 2-aPu fluorescence intensity increases initially (in the first step) but does not decrease at longer times. Therefore, if the G-base is everted from the DNA-chain, the void should be filled with the amino acids of hOGG1. Therefore, we conclude that under the experimental conditions of this study, where the equilibrium between free and DNA-bound enzyme is not kinetically restricted, the non-damaged G-base does not form a stable flipped out complex with the enzyme (as in the case of X-ray analysis [21]), although such a complex can be formed transiently.

Thus, the analysis of the kinetic data obtained in this study permits to track the participation of single amino acids of hOGG1 in the reaction pathway. This provides a better understanding of the sequence of steps in the molecular mechanism of hOGG1 lesion recognition (Scheme 3). It was demonstrated that Lys-249 plays an important role in the early step of the damaged base binding and flipping out. The kinetic data support the idea that hOGG1 possesses "uncoupled" catalytic activity [16] where Asp-268 is responsible for the hydrolysis of the N-glycosidic bond, while Lys-249 is a key amino acid in the sugar–phosphate bond cleavage (β-elimination reaction). We showed that His-270 participates in DNA-binding and in the oxoG flipping out process. We proposed that Tyr-203 plays a role as "lesion-sensor needle" in the discrimination between normal and damaged bases. The features of the non-specific base binding were specified.

Acknowledgements

We thank Prof. Robert Kaptein for comments and help in preparing the manuscript.

This study was supported by the program of the Russian Academy of Sciences "Molecular & Cell Biology" (No. 6–11), the Grants from the Russian Foundation for Basic Research (13-04-00013 and 12-04-31066) and Russian Ministry of Education and Science (SS-64.2012.4, SP-4012.2013.4, 8092, 8473 and 14.B37.21.0195), the Grant from the Russian Government to support leading scientists (No. 11.G34.31.0045), as well as the Grants from Agence Nationale pour la Recherche [ANR Blanc 2010 Project ANR-09-GENO-000 to M.S.] (http://www.agence-nationale-recherche.fr), Centre National de la Recherche Scientifique (http://www.cnrs.fr) [PICS N5479-Russie to M.S.], Electricité de France Contrat Radioprotection (http://www.edf.fr) [RB 2013 to M.S.] and Fondation de France (http://www.fondationdefrance.org) [#2012 00029161 to A.A.I.].

Appendix A. Supplementary data

Supplementary data to this article can be found online at http://dx.doi.org/10.1016/j.bbagen.2013.09.035.

References

[1] S.S. Wallace, Biological consequences of free radical-damaged DNA bases, Free Radic. Biol. Med. 33 (2002) 1–14.
[2] M.D. Evans, M. Dizdaroglu, M.S. Cooke, Oxidative DNA damage and disease: induction, repair and significance, Mutat. Res. 567 (2004) 1–61.
[3] T.A. Rosenquist, D.O. Zharkov, A.P. Grollman, Cloning and characterization of a mammalian 8-oxoguanine DNA glycosylase, Proc. Natl. Acad. Sci. U. S. A. 94 (1997) 7429–7434.
[4] D.O. Zharkov, T.A. Rosenquist, S.E. Gerchman, A.P. Grollman, Substrate specificity and reaction mechanism of murine 8-oxoguanine-DNA glycosylase, J. Biol. Chem. 275 (2000) 28607–28617.
[5] P.A. van der Kemp, D. Thomas, R. Barbey, R. de Oliveira, S. Boiteux, Cloning and expression in *Escherichia coli* of the OGG1 gene of *Saccharomyces cerevisiae*, which codes for a DNA glycosylase that excises 7,8-dihydro-8-oxoguanine and 2,6-diamino-4-hydroxy-5-N-methylformamidopyrimidine, Proc. Natl. Acad. Sci. U. S. A. 93 (1996) 5197–5202.
[6] J.P. Radicella, C. Dherin, C. Desmaze, M.S. Fox, S. Boiteux, Cloning and characterization of hOGG1, a human homolog of the OGG1 gene of *Saccharomyces cerevisiae*, Proc. Natl. Acad. Sci. U. S. A. 94 (1997) 8010–8015.
[7] M. Bjoras, L. Luna, B. Johnsen, E. Hoff, T. Haug, T. Rognes, E. Seeberg, Opposite base-dependent reactions of a human base excision repair enzyme on DNA containing 7,8-dihydro-8-oxoguanine and abasic sites, EMBO J. 16 (1997) 6314–6322.
[8] S. Shibutani, M. Takeshita, A.P. Grollman, Insertion of specific bases during DNA synthesis past the oxidation-damaged base 8-oxodG, Nature 349 (1991) 431–434.
[9] K. Asagoshi, T. Yamada, H. Terato, Y. Ohyama, Y. Monden, T. Arai, S. Nishimura, H. Aburatani, T. Lindahli, H. Ide, Distinct repair activities of human 7,8-dihydro-8-oxoguanine DNA glycosylase and formamidopyrimidine DNA glycosylase for formamidopyrimidine and 7,8-dihydro-8-oxoguanine, J. Biol. Chem. 275 (2000) 4956–4964.
[10] P.M. Girard, N. Guibourt, S. Boiteux, The Ogg1 protein of *Saccharomyces cerevisiae*: a 7,8-dihydro-8-oxoguanine DNA glycosylase/AP lyase whose lysine 241 is a critical residue for catalytic activity, Nucleic Acids Res. 25 (1997) 3404–3411.
[11] H.M. Nash, R. Lu, W.S. Lane, G.L. Verdine, The critical active-site amine of the human 8-oxoguanine DNA glycosylase, hOgg1: direct identification, ablation and chemical reconstitution, Chem. Biol. 4 (1997) 693–702.
[12] M.M. Thayer, H. Ahern, D. Xing, R.P. Cunningham, J.A. Tainer, Novel DNA binding motifs in the DNA repair enzyme endonuclease III crystal structure, EMBO J. 14 (1995) 4108–4120.
[13] J. Labahn, O.D. Schärer, A. Long, K. Ezaz-Nikpay, G.L. Verdine, T.E. Ellenberger, Structural basis for the excision repair of alkylation-damaged DNA, Cell 86 (1996) 321–329.
[14] Y. Guan, R.C. Manuel, A.S. Arvai, S.S. Parikh, C.D. Mol, J.H. Miller, R.S. Lloyd, J.A. Tainer, MutY catalytic core, mutant and bound adenine structures define specificity for DNA repair enzyme superfamily, Nat. Struct. Biol. 5 (1998) 1058–1064.
[15] D.P. Norman, S.J. Chung, G.L. Verdine, Structural and biochemical exploration of a critical amino acid in human 8-oxoguanine glycosylase, Biochemistry 42 (2003) 1564–1572.
[16] B. Dalhus, M. Forsbring, I.H. Helle, E.S. Vik, R.J. Forstrom, P.H. Backe, I. Alseth, M. Bjoras, Separation-of-function mutants unravel the dual-reaction mode of human 8-oxoguanine DNA glycosylase, Structure 19 (2011) 117–127.
[17] S.D. Bruner, D.P. Norman, G.L. Verdine, Structural basis for recognition and repair of the endogenous mutagen 8-oxoguanine in DNA, Nature 403 (2000) 859–866.
[18] M. Bjoras, E. Seeberg, L. Luna, L.H. Pearl, T.E. Barrett, Reciprocal "flipping" underlies substrate recognition and catalytic activation by the human 8-oxo-guanine DNA glycosylase, J. Mol. Biol. 317 (2002) 171–177.
[19] A. Banerjee, W. Yang, M. Karplus, G.L. Verdine, Structure of a repair enzyme interrogating undamaged DNA elucidates recognition of damaged DNA, Nature 434 (2005) 612–618.
[20] C.T. Radom, A. Banerjee, G.L. Verdine, Structural characterization of human 8-oxoguanine DNA glycosylase variants bearing active site mutations, J. Biol. Chem. 282 (2007) 9182–9194.
[21] C.M. Crenshaw, K. Nam, K. Oo, P.S. Kutchukian, B.R. Bowman, M. Karplus, G.L. Verdine, Enforced presentation of an extrahelical guanine to the lesion recognition pocket of human 8-oxoguanine glycosylase, hOGG1, J. Biol. Chem. 287 (2012) 24916–24928.
[22] N.A. Kuznetsov, V.V. Koval, D.O. Zharkov, G.A. Nevinsky, K.T. Douglas, O.S. Fedorova, Kinetics of substrate recognition and cleavage by human 8-oxoguanine-DNA glycosylase, Nucleic Acids Res. 33 (2005) 3919–3931.
[23] N.A. Kuznetsov, V.V. Koval, G.A. Nevinsky, K.T. Douglas, D.O. Zharkov, O.S. Fedorova, Kinetic conformational analysis of human 8-oxoguanine-DNA glycosylase, J. Biol. Chem. 282 (2007) 1029–1038.
[24] K.A. Johnson, Advances in transient-state kinetics, Curr. Opin. Biotechnol. 9 (1998) 87–89.
[25] P. Kuzmic, Program DYNAFIT for the analysis of enzyme kinetic data: application to HIV proteinase, Anal. Biochem. 237 (1996) 260–273.
[26] P.A. van der Kemp, J.B. Charbonnier, M. Audebert, S. Boiteux, Catalytic and DNA-binding properties of the human Ogg1 DNA N-glycosylase/AP lyase: biochemical exploration of H270, Q315 and F319, three amino acids of the 8-oxoguanine-binding pocket, Nucleic Acids Res. 32 (2004) 570–578.
[27] N. Guibourt, B. Castaing, P.A. Van Der Kemp, S. Boiteux, Catalytic and DNA binding properties of the ogg1 protein of *Saccharomyces cerevisiae*: comparison between the wild type and the K241R and K241Q active-site mutant proteins, Biochemistry 39 (2000) 1716–1724.
[28] D.P. Norman, S.D. Bruner, G.L. Verdine, Coupling of substrate recognition and catalysis by a human base-excision DNA repair protein, J. Am. Chem. Soc. 123 (2001) 359–360.
[29] M. Audebert, J.P. Radicella, M. Dizdaroglu, Effect of single mutations in the OGG1 gene found in human tumors on the substrate specificity of the Ogg1 protein, Nucleic Acids Res. 28 (2000) 2672–2678.
[30] F. Faucher, S.S. Wallace, S. Doublie, Structural basis for the lack of opposite base specificity of *Clostridium acetobutylicum* 8-oxoguanine DNA glycosylase, DNA Repair (Amst) 8 (2009) 1283–1289.
[31] V.V. Koval, N.A. Kuznetsov, A.A. Ishchenko, M.K. Saparbaev, O.S. Fedorova, Real-time studies of conformational dynamics of the repair enzyme *E. coli* formamidopyrimidine-DNA glycosylase and its DNA complexes during catalytic cycle, Mutat. Res. 685 (2010) 3–10.
[32] A.R. Dunn, N.M. Kad, S.R. Nelson, D.M. Warshaw, S.S. Wallace, Single Qdot-labeled glycosylase molecules use a wedge amino acid to probe for lesions while scanning along DNA, Nucleic Acids Res. 39 (2011) 7487–7498.
[33] M. Rogacheva, A. Ishchenko, M. Saparbaev, S. Kuznetsova, V. Ogryzko, High resolution characterization of formamidopyrimidine-DNA glycosylase interaction with its substrate by chemical cross-linking and mass spectrometry using substrate analogs, J. Biol. Chem. 281 (2006) 32353–32365.
[34] S.D. Williams, S.S. David, Formation of a Schiff base intermediate is not required for the adenine glycosylase activity of *Escherichia coli* MutY, Biochemistry 38 (1999) 15417–15424.
[35] D.O. Zharkov, R. Gilboa, I. Yagil, J.H. Kycia, S.E. Gerchman, G. Shoham, A.P. Grollman, Role for lysine 142 in the excision of adenine from A:G mispairs by MutY DNA glycosylase of *Escherichia coli*, Biochemistry 39 (2000) 14768–14778.
[36] T. Hollis, Y. Ichikawa, T. Ellenberger, DNA bending and a flip-out mechanism for base excision by the helix–hairpin–helix DNA glycosylase, *Escherichia coli* AlkA, EMBO J. 19 (2000) 758–766.
[37] S. Lee, G.L. Verdine, Atomic substitution reveals the structural basis for substrate adenine recognition and removal by adenine DNA glycosylase, Proc. Natl. Acad. Sci. U. S. A. 106 (2009) 18497–18502.